NEUROIMAGE **7,** 352–367 (1998)
ARTICLE NO. NI980330

Biophysical Linkage between MRI and EEG Amplitude in Closed Head Injury

R. W. Thatcher,*,†,[1] C. Biver,† R. McAlaster,† M. Camacho,*,† and A. Salazar†

**Bay Pines VA Medical Center, Bay Pines, Florida 33744; and †Defense and Veterans Head Injury Program, Washington, DC 20307*

Received September 24, 1997

Nuclear magnetic resonance of brain water proton (^{1}H) T2 relaxation times and measures of absolute amplitude of EEG were obtained from 19 closed head injured patients. The relationship between EEG and T2 relaxation time differed as a function of both EEG frequency and gray matter versus white matter. White matter T2 relaxation time was positively correlated with increased EEG amplitude in the δ frequency band (0.5–3.5 Hz). In contrast, lengthened gray matter T2 relaxation time was inversely correlated with EEG amplitude in the α and β frequency bands (7–22 Hz). These findings are consistent with clinical EEG studies in which white matter lesions are related to increased EEG δ amplitude and gray matter lesions are related to decreased EEG α and β frequency amplitude. Estimates of the severity of injury were obtained by neuropsychological measurements, in which lengthened T2 relaxation times in both the neocortical gray and white matter were correlated with diminished cognitive function. Decreased EEG β and α amplitude and increased EEG δ amplitude were also correlated with diminished cognitive function. The findings imply a biophysical linkage between the state of protein–lipid structures of the brain as measured by the MRI and the scalp-recorded EEG. © 1998 Academic Press

Key Words: **EEG; MRI; T2 relaxation times; cognition; traumatic brain injury.**

INTRODUCTION

Conventional visual MRI examination of the brains of closed head injured (CHI) patients frequently underestimates the true extent of pathology (Adams *et al.,* 1989; Graham *et al.,* 1993; Smith *et al.,* 1995). For example, approximately 15 to 40% of moderate to severe CHI patients exhibited visually detectable pathology in the MRI, while in autopsy, microscopic examinations of these same patients demonstrated that approximately 90% of patients have gray matter contusions as well as shear force injuries diffusely located within the cortical gray and white matter (Gentry, 1990, 1994; Gentry *et al.,* 1988). In contrast to visual examination of the MRI, computerized electroencephalography referred to as QEEG has been shown to be greater than 90% accurate in the detection of even mild CHI (Thatcher *et al.,* 1989, 1991). However a weakness of QEEG is the lack of physiological and anatomical specificity because many changes in the chemistry and physiology of neurons and glia can affect the EEG power spectrum (Nunez, 1981, 1995; Lopes da Silva, 1991). A recent quantitative MRI study demonstrated a shift in the water proton relaxation times within the brain of closed head injured patients (Thatcher *et al.,* 1997). This study suggested a possible integration of EEG with MRI by integrating EEG with the biophysical aspects of conventional clinical MRI, namely, water proton (^{1}H) nuclear magnetic resonance (^{1}H NMR). Such an integration may strengthen both the conventional clinical MRI and the EEG since the weak sensitivity and high physiological resolution of the MRI may be mutually strengthened by the high sensitivity but weak physiological resolution of the EEG. For these reasons, in the present study we evaluated the hypothesis that there is a quantifiable relationship between ^{1}H NMR relaxation times of the brain, scalp-recorded EEG, and cognitive function in CHI patients.

METHODS

Subjects

The patients were 18 males and 1 female and ranged in age from 19 to 48 years (mean age = 32.6 years, SD = 10.6). The patients were tested during the post-acute to chronic period following injury (time from injury to EEG and MRI evaluation ranged from 10 days to 11 years with a mean of 1.7 years). Severity of injury

[1] To whom reprint requests should be addressed at Research and Development Service—151, Veterans Administration Medical Center, Bay Pines, FL 33744.

1053-8119/98 $25.00

varied from moderate to severe, but all of the patients were conscious and alert with varying amounts of completed rehabilitation at the time of testing (Thatcher *et al.,* 1997). The patients were tested as part of a Defense and Head Injury Program (DVHIP). All of the EEGs, MRIs, and neuropsychological tests were obtained at the J. A. Haley VA Hospital in Tampa, Florida. Only CHI patients were included in the study. All of the patients were diagnosed using ICD-9 (i.e., intracranial injury excluding those with penetrating head wounds or codes within the 850 to 854 categories). Approximately 64% of the patients were motor-vehicle accident victims, 16% were victims of industrial or home accidents, and 20% were victims of violent crime.

Neuropsychological Testing

Typically, the severity of closed head injury is judged by: (1) length of loss of consciousness (LOC) and/or (2) length of posttraumatic amnesia (PTA) and/or (3) the Glasgow Coma Score (GCS). It is known that the GCS is often not obtained by emergency personnel. Accurate measures of PTA require a trained professional to administer tests, and LOC is often unknown by the accident victims themselves. Thus, estimates of severity of head injury are prone to error. In the present study the severity of injury was measured by neuropsychological tests that were administered when the patients were admitted into the DVHIP program, which was often many months postinjury (mean = 1.7 years). Neuropsychological tests only measure the level of cognitive function at the time of the test, thus the exact contribution of the head injury to the patient's current neuropsychological function is unknown. Nonetheless, the neuropsychological tests used in the present study are the standard tests used today to evaluate closed head injury in the posttraumatic period (Levin *et al.,* 1982). Thus, the neuropsychological tests in the present study are used only to evaluate the current level of cognitive function and in this sense the neuropsychological variables are only indirect measures of severity of injury. No attempt will be made to explain differences between specific neuropsychological tests as they relate to EEG and MRI. This must await a study of a larger sample of subjects. A total of seven neuropsychological tests were administered to the patients, in which some data were missing because of unreliable responses or a general inability to complete the test. A principal components analysis with a varimax rotation was performed to determine the dimensionality of the neuropsychological measures. Four varimax factors accounted for 78.6% of the variance. Among the highest loading variables (e.g., >0.8) on the factors were the number of stimulus cues given in the Boston Naming Test, Percentile Rank for Digit Span Backward (WISC-R), Digit Span Raw Score (WISC-R), and the List A total trials 1–5 for the California Verbal Learning Test.

EEG Recording

Power spectral analysis was implemented on 3- to 5-min segments of eyes-closed resting EEG recorded from 16 scalp locations using the left ear lobe as a reference in all 19 CHI patients. EKG and eye movement electrodes were applied to monitor artifact and all EEG records were edited to remove any visible artifact. The amplifier bandwidths were nominally 0.5 to 30 Hz, the outputs being 3 dB down at these frequencies. Three to five minutes of eyes-closed EEG was digitized at 100 Hz and then spectral analyzed using a complex demodulation procedure (Otnes and Enochson, 1972; Barlow, 1993). The final edited EEG epoch length that was spectrally analyzed varied from 49.5 to 125 s (mean = 87 s). Absolute EEG amplitude was computed from the 16 scalp locations in the δ (0.5 to 3.5 Hz), θ (3.5 to 7 Hz), α (7.5 to 13 Hz), and β (13 to 22 Hz) frequency bands. The frequency bands, including the center frequencies (f_c) and one-half power values (B) were δ (0.5 to 3.5 Hz; $f_c = 2.0$ Hz; $B = 1.0$), θ (3.5 to 7.0 Hz; $f_c = 4.25$ Hz; $B = 3.5$ Hz), α (7.0 to 13.0 Hz; $f_c = 9.0$ Hz; $B = 6.0$ Hz), and β (13 to 22 Hz; $f_c = 19$ Hz; $B = 14.0$ Hz). EEG amplitude was computed as the square root of power. The mathematical details of the analyses are provided in Otnes and Enochson (1972), Thatcher *et al.* (1989, 1991), and Thatcher (1995).

MRI Acquisition

The MR images were acquired using a Picker 1.5-T scanner with a double-spin echo for T2 and proton density and a T1-weighted spin–echo sequence. All acquisitions were precisely the same for all subjects and used 3-mm slices with no gaps between slices. The double-echo proton density (PD) and T2 sequences were interleaved and had a TR = 3000 ms with TEs of 30 and 90 ms, FOV of 24 cm, a 90° flip angle, and a 256×192 matrix. The T1-weighted sequence used TR = 883 ms with a TE = 20 ms, FOV = 24 cm, a 90° flip angle, and a 256×192 matrix. A multispectral k-Nearest Neighbor manual segmentation and classification algorithm and a multispectral fuzzy c-means (FCM) algorithm were used for gray matter, white matter, and CSF segmentation (Clarke *et al.,* 1995; Bezdek *et al.,* 1993; Bensaid *et al.,* 1994). This involved the use of a brain mask that was manually traced for each axial proton density image via a polygon tracing algorithm isolating the brain from skull and dura. To minimize error and to improve segmentation accuracy a validity-guided reclustering algorithm was used on each FCM segmented slice (Bensaid *et al.,* 1994). Every segmented slice was manually classified via a graphical user interface into

five classes: background, white matter, gray matter, CSF, and other. Slice 1 or the lowest starting slice was landmark identified as being at the level of the genu of the corpus callosum, the septum pellucidum, and the forceps major and minor. As illustrated in Fig. 1, slices 1 to 15 represent a contiguous spatial volume of 4.5 cm (i.e., 3 mm $\times$ 15 = 4.5 cm) beginning from the starting landmark axial slice and extending to the top of the cortex. For further details see Thatcher *et al.* (1997).

Cortical gray matter is defined as neocortical neurons, glia, and supporting cellular constituents located within the nonmyelinated part of the cerebral mantel, beginning at the corpus callosum starting axial slice (Thatcher *et al.,* 1997) and extending vertically to the top of the neocortex. Cortical white matter is defined as the myelinated axons located in the same axial planes and volumes as the neural cell bodies located in the neocortical gray matter. In this study, white matter is referred to as "cortical white matter" because it is dominated by the neocortical lobar white matter and the numerous corticocortical association fibers (Carpender and Sutin, 1983). This nomenclature is justified in studies by Braitenberg and Schuz (1991) and others (Nunez, 1981, 1995; Braitenberg, 1972; 1978) which show that only approximately 5% of myelinated fibers originate from the subcortex, while approximately 95% of myelinated axons within the cortical white matter originate and terminate within the neocortex.

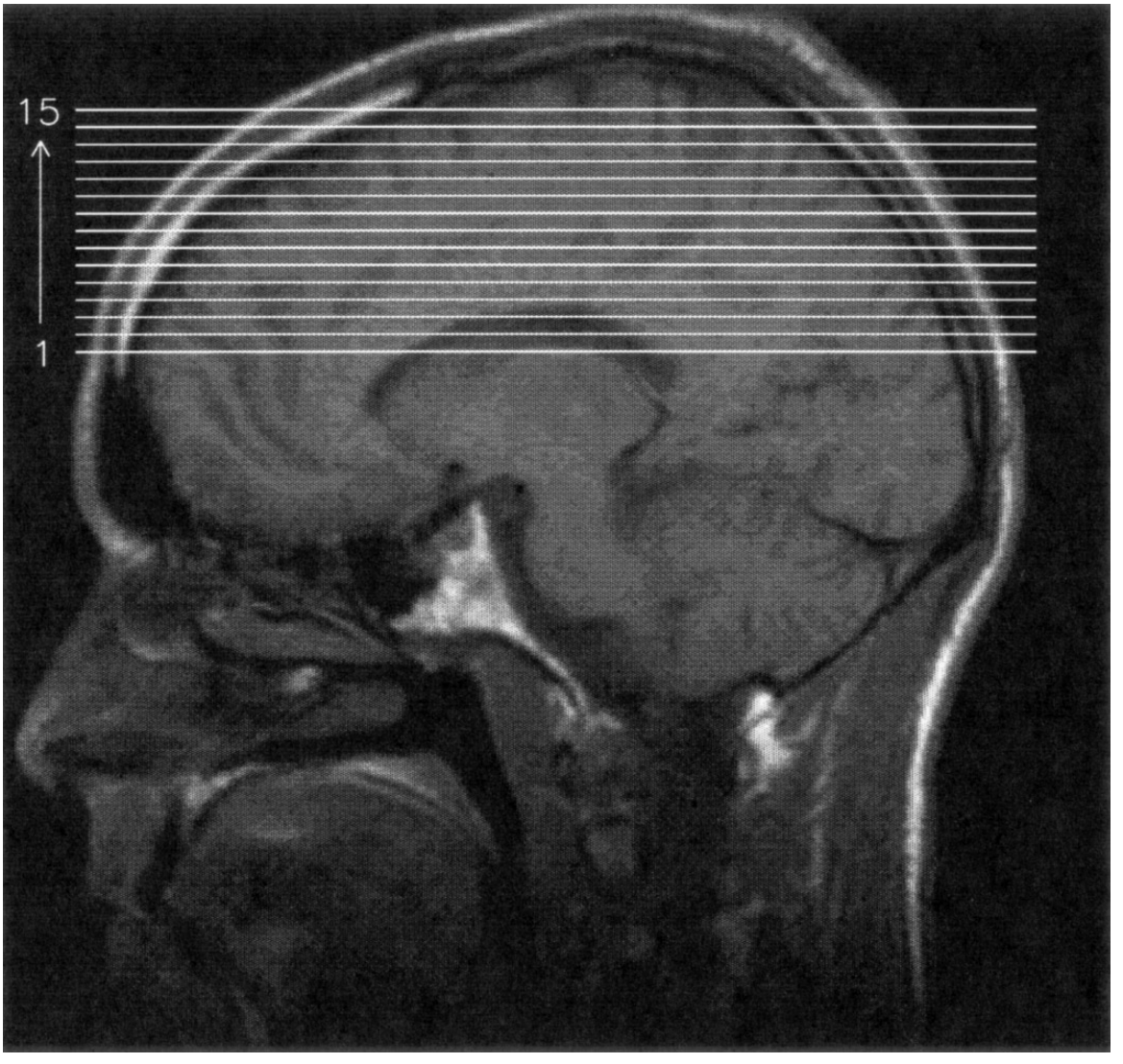

FIG. 1. Illustration of slice locations and cortical volume. Illustration of the locations of the 15 axial 3-mm slices used in the present study. The location of the first axial slice was the same for all subjects. The lowest or starting slice was identified at the level of the genu of the corpus callosum, the septum pellucidum, and the forceps major and minor (see Thatcher *et al.,* 1997 for further details). Gray matter and white matter were segmented and classified for each axial slice. The mode of T2 relaxation time was determined for each slice within the segmented gray and white matter.

Calculations of ^{1}H NMR T2 Relaxation Times

We used the solutions of the Bloch equations (Bloch, 1946) to calculate T1, PD, and T2 (Dixon and Ekstrand, 1982; Kjos *et al.,* 1985; Darwin *et al.,* 1986; Hickley *et al.,* 1986; Mills *et al.,* 1984). According to this solution, MR signal intensity (I) is related to ^{1}H relaxation times by $I = KN(1 - e^{-TR/T1})e^{-TR/T2}$, where K is the velocity and scaling constants, N is the hydrogen spin density, TR is the repetition time, TE is the echo time, T1 is the spin–lattice relaxation time, and T2 is the spin–spin relaxation time. T2 was solved analytically using the PD and T2 images acquired in an interleaved manner in which the corresponding TR values were equal, TR $\gg$ TE, and molecular velocity and scaling = 1. The equation was

$$T2 = \frac{TE_{PD} - TE_{T2}}{\ln(I_{T2}/I_{PD})}, \quad (1)$$

where I_{T2} and I_{PD} were the pixel intensities from the respective T2 and PD images (mathematical details are provided in the Appendix).

T1 relaxation time was also computed; however, this study focuses on T2 because T1 relaxation time required an iterative solution and T1 assumes spatial registration with the PD and T2 slice, which may or may not be exact. Finally, T1 or the spin–lattice interactions have a much slower relaxation time than T2 spin–spin interactions, resulting in a less temporal resolution of the average time that water protons reside in cytoplasm, myelin, or extracellular space (see Fig. 9).

The T2 gray matter and white matter histogram distributions within a given 3-mm slice were always unimodal but sometimes skewed or kurtotic. The rationale for the use of the mode, in contrast to the mean, is that the mode represents the most frequently occurring value within a sample. Errors in segmentation, which primarily occur at the borders of tissue classes, are minimized by the use of the mode. Thus, in order to use a reliable and simple measure, the mode of the frequency distribution of T2 for the segmented gray matter and white matter was calculated for each axial slice and used as the MRI independent variable in this study.

RESULTS

Gray and White Matter Distribution of T2 Relaxation Times

The anatomical distribution of T2 relaxation times in the cortical gray and white matter from a representative MRI slice at the level of the superior central sulcus and middle frontal gyrus (slice 10 or approx 3.0 cm above the corpus callosum) is shown in the top row of Fig. 2. Individual pixels were color coded to correspond to relaxation time ranges for both the segmented gray matter and the segmented white matter. It can be seen that in general T2 relaxation times are longer in the gray matter than in the white matter, i.e., more red and orange colors. Spatial inhomogeneities in the distribution of T2 relaxation times are also evident in Fig. 2, especially in the white matter where shorter T2 relaxation times (green and blue) were present in the frontal lobes in comparison to the posterior and midcortical regions.

The raw (black dots) and Savitzgy and Golay (1964) smoothed distributions (red line) of T2 relaxation times within the cortical gray and white matter are shown in the bottom row of Fig. 2. It can be seen that the distributions are positively skewed but relatively well behaved with longer relaxation times in the gray matter in comparison to the white matter. As mentioned previously, use of the mode of the T2 distribution helps minimize, but not eliminate, errors in segmentation and classification (Clarke *et al.,* 1995).

Correlations between EEG Amplitude and T2 Relaxation Times

A multivariate analysis of variance (MANOVA) was conducted on the Fischer transformed correlation matrix of gray and white matter T2 relaxation times and EEG amplitude in the δ, θ, α, and β frequency bands (Velleman, 1995; Cohen and Cohen, 1983). The overall main effect of EEG frequency was statistically significant ($df = 1/7$, $F = 597.94$, $P < 0.0001$) with statistically significant T2 relaxation time factors being the gray and white matter and the frequency of EEG amplitude. Bonferroni post hoc tests revealed significantly higher correlations between EEG δ frequency amplitude for white matter T2 relaxation time in comparison to the gray matter T2 relaxation time ($P < 0.0001$) and significantly higher correlations between EEG α and β frequency amplitude for gray matter T2 relaxation time in comparison to the white matter T2 relaxation time ($P < 0.0001$). To explore these findings in more detail individual regression analyses were conducted in which EEG amplitude and the log of EEG amplitude were the dependent variables and T2 relaxation times were the independent variables. In nearly every case, the log of EEG amplitude exhibited higher correlations than the untransformed EEG amplitude values. A summary of the number and sign of statistically significant correlations ($r \geq 0.45$, $P \leq 0.05$) between T2 relaxation time modes and the log of EEG amplitude in the δ (0.5–3.5 Hz), θ (3.5–7 Hz), α (7–13 Hz), and β (13–22 Hz) frequency bands is shown in Table 1. For referential purposes, in a given EEG frequency band, 22 correlations would be expected to be significant at $P < 0.05$ by chance alone (i.e., 15 slices $\times$ 16 electrode locations = 240 $\times$ 0.05 = 12). The MANOVA results established the main statistically

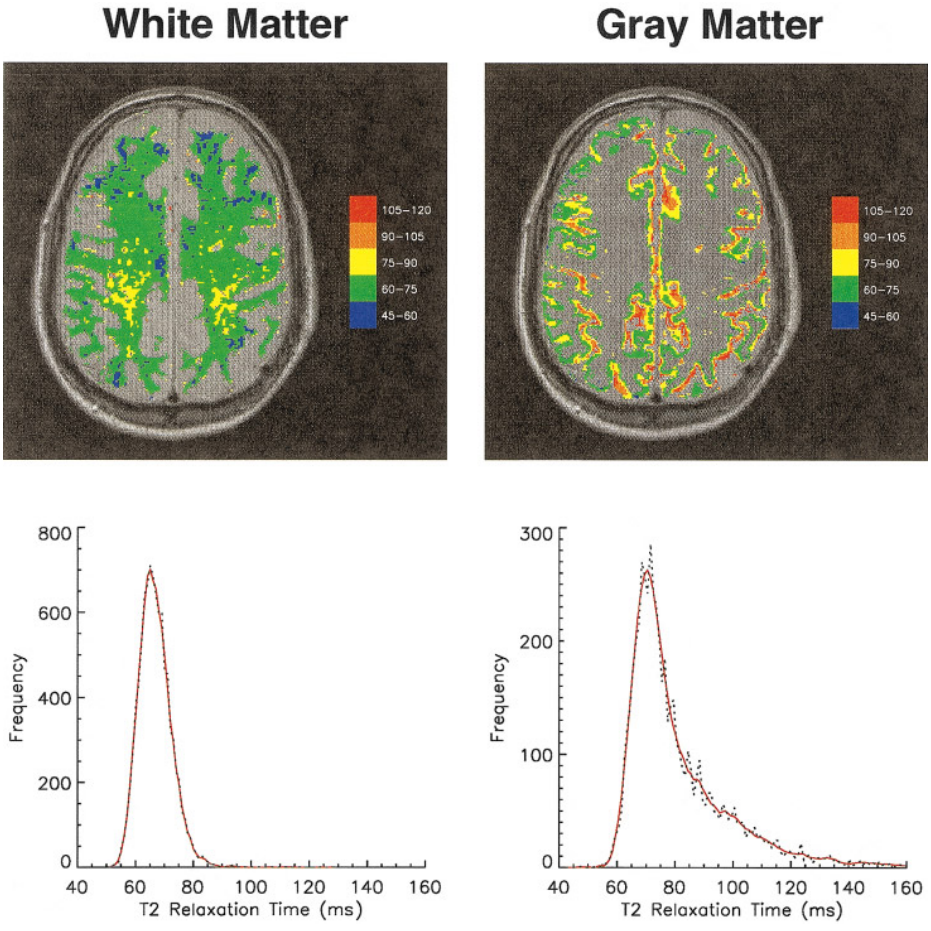

FIG. 2. T2 relaxation times. Representative examples of T2 color-coded MRI pixels in a 3-mm proton density axial slice. Segmented white matter T2 relaxation times are on the top left and segmented gray matter T2 relaxation times are on the top right from slice 10 of a TBI patient. Axial slice 10 is located approximately 3.0 cm above the corpus callosum. Gray matter T2 relaxation times are relatively spatially uniform with long T2 relaxation times (e.g., red color) distributed throughout the slice. In contrast, white matter T2 relaxation times are spatially heterogeneous with comparatively shorter relaxation times than in the gray matter. The T2 relaxation time histograms from the segmented white matter (left) and gray matter (right) are at the bottom. The dots are the actual T2 values and the red line is the Savitzky and Golay (1964) fit of the distributions. The mode of the smoothed T2 histogram for each axial slice was the independent variable in this study. Methods of computing T2 relaxation times from a conventional MR image are described in the text and the Appendix.

significant relationships between T2 relaxation time and EEG amplitude. The purpose of Table 1 is to show the categorical "effect size" (Cohen and Cohen, 1983) of the T2 MRI measure with the EEG amplitude. For example, a large effect size was present in the gray matter to β frequency band where of a total of 240 correlations 143 were positive versus zero negative correlations. Table 1 also shows that the sign of the correlation between T2 and EEG amplitude varied as a function of frequency. For example, the correlations were positive in the δ frequency band but negative in the α and β frequency bands.

Statistically significant differences in the sign or direction of the correlations were present both in the T2 gray matter and in the T2 white matter in that there were more negative correlations than positive correlations in the gray matter ($\chi^2 = 172.64/1\ df$; $P < 0.0001$) and more positive correlations than negative correlations in the white matter ($\chi^2 = 17.6/1\ df$; $P = 0.0001$). There was also a larger number of significant T2 gray matter correlations in comparison to T2 white matter correlations ($\chi^2 = 47.68/1\ df$; $P < 0.0001$).

Figure 3 shows representative examples of the scattergram plots of the relationships between T2 relaxation times and the log of the absolute amplitude of EEG in the β frequency band (13 to 22 Hz). It can be seen in Fig. 3 that there is some scatter around the regression line and the correlations are in a middle effect size range, e.g., 0.55 to 0.7 (Cohen and Cohen, 1983). Most importantly, as Table 1 and Fig. 3 show, there is a consistent and distinct inverse relationship between T2 relaxation time and the higher frequencies

TABLE 1

Number and Sign of Significant Correlations ($P < 0.05$) between Gray Matter and White Matter T2 Relaxation Times and Log of EEG Amplitude[a]

	Δ	Θ	*A*	*B*
Gray				
+	12	0	0	0
−	0	5	87	143
White				
+	31	2	0	0
−	0	1	23	67

[a] Twelve statistically significant correlations ($P < 0.05$) in each cell are expected to occur by chance alone.

of the EEG (e.g., 7 to 22 Hz), that is, as the gray matter T2 lengthens, EEG higher frequency amplitudes decrease.

A different relationship was observed between cortical white matter T2 and the EEG frequency spectrum. As seen in Table 1 and Fig. 4, lengthened white matter T2 was related to an increase in amplitude of the EEG δ frequency band (0.5–3.5 Hz). This positive relationship was never observed between the gray matter T2 and the EEG frequency spectrum. The increased δ EEG amplitude and white matter T2 effect tended to be weaker than the gray matter T2 and increased β amplitude effect.

Topographic Relations between T2 Relaxation Times and EEG Amplitude

In order to reduce the total number of regression analyses, T2 relaxation times were averaged across the 15 slices for each subject. The average T2 values for the entire 4.5-cm cortical volume (i.e., starting at the corpus callosum and extending to the upper cortex), rather than slice by slice, were then correlated with the 16 channels of EEG amplitude. A topographic view of the number and sign of statistically significant correlations between T2 relaxation time modes and the log of EEG amplitude in the δ, θ, α, and β frequency bands is shown in Fig. 5. In Fig. 5, the solid circles represent negative correlations and the striped circles represent positive correlations, while the sizes of the circles represent the level of statistical significance. It can be seen that the β and α frequencies exhibited negative

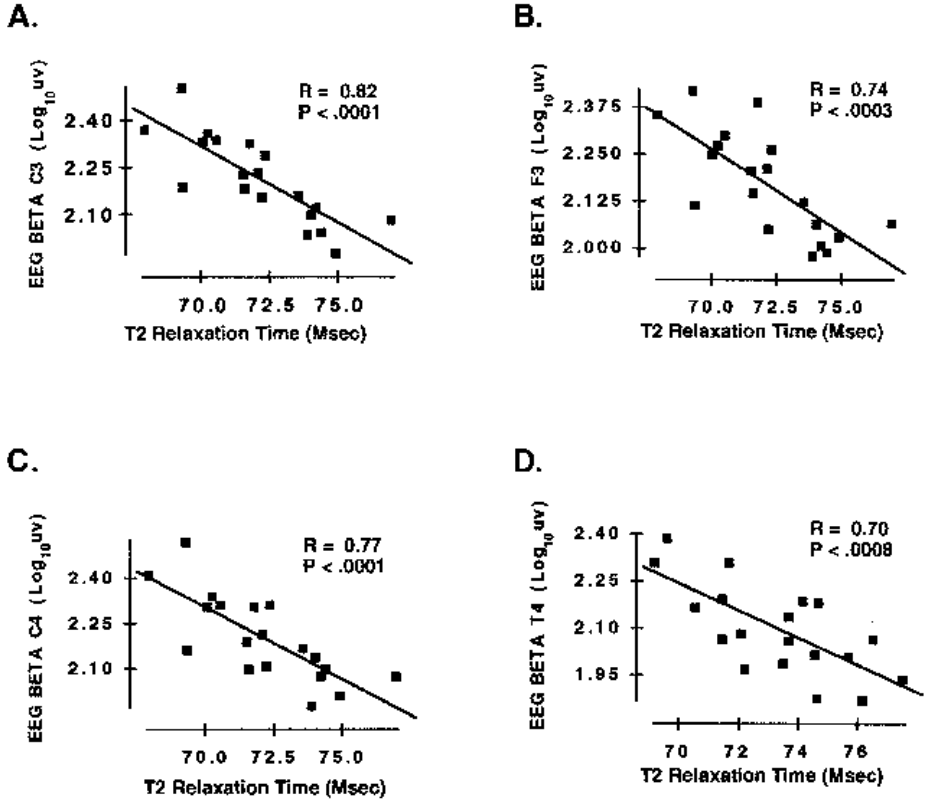

FIG. 3. T2 gray matter and EEG β frequency scattergrams. Representative scattergrams between the $\log_{10}$ EEG amplitude in the β frequency band (13–22 Hz) (*y* axis) and T2 relaxation times (*x* axis). (A) Scattergram from slice 10 gray matter (*x* axis) and C3 β EEG amplitude (*y* axis). (B) Scattergram from slice 9 white matter (*x* axis) and F3 β EEG amplitude (*y* axis). (C) Scattergram from slice 10 gray matter (*x* axis) and C4 β EEG amplitude (*y* axis). (D) Scattergram from slice 9 white matter (*x* axis) and T4 β EEG amplitude (*y* axis).

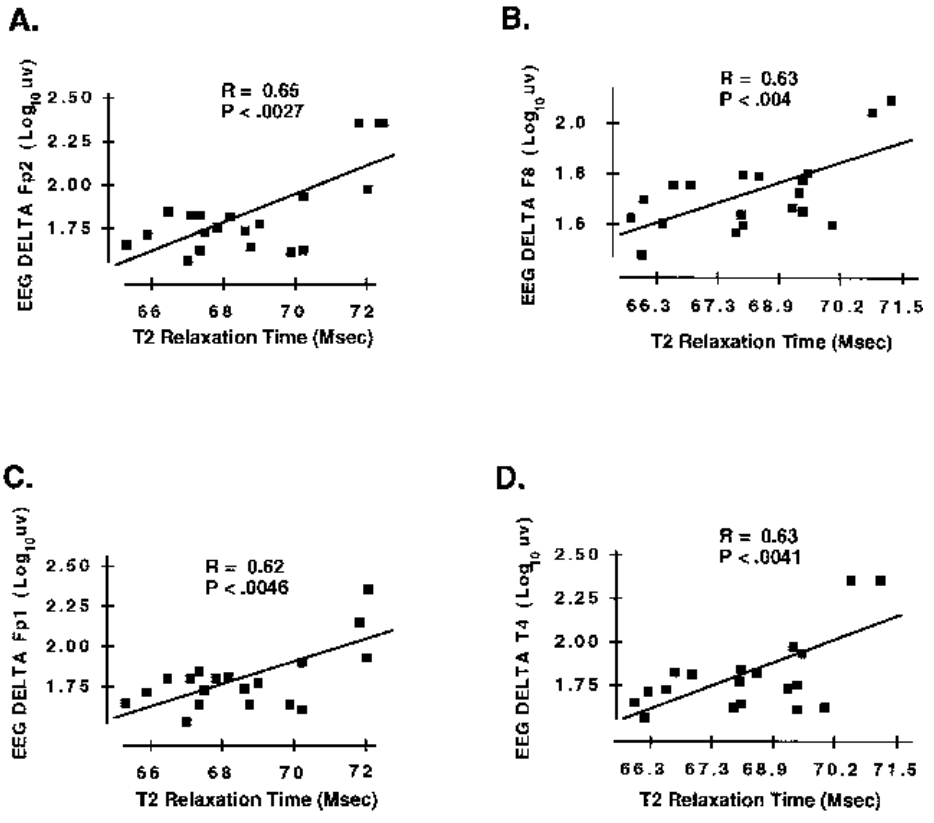

FIG. 4. T2 white matter and EEG δ frequency scattergrams. Representative scattergrams between the $\log_{10}$ EEG amplitude in the δ frequency band (0.5–3.5 Hz) (*y* axis) and T2 relaxation times (*x* axis). (A) Scattergram from slice 10 gray matter (*x* axis) and F2 δ EEG amplitude (*y* axis). (B) Scattergram from slice 9 white matter (*x* axis) and F8 δ EEG amplitude (*y* axis). (C) Scattergram from slice 10 gray matter (*x* axis) and F1 δ EEG amplitude (*y* axis). (D) Scattergram from slice 9 white matter (*x* axis) and T4 δ EEG amplitude (*y* axis).

correlations to the gray matter T2 while the δ frequency band exhibited positive correlations to white matter T2. There also appeared to be a different anatomical relationship between the EEG frequency spectrum and the gray and white matter T2 relaxation times. For example, white matter T2 was most strongly related to the frontal poles (e.g., Fp1 and Fp2) in the δ frequency band while gray matter T2 was most strongly related to the lateral frontal prefrontal (F3/4, C3/4) and temporal cortex (T3/4).

Anatomical Distribution of Correlations between T2 Relaxation Time and EEG Amplitude

The spatial distributions of mean correlation between the T2 relaxation time mode and the EEG frequency in the gray and white matter across 15 axial MRI slices are shown in Fig. 6. Mean T2 and EEG frequency correlations were similar in the gray and white matter with δ frequency positively correlated and α and β frequencies negatively correlated. The θ EEG frequency was intermediate between δ and β and relatively poorly correlated to T2 with average values near to 0. Different spatial distributions of correlation between gray and white matter were present with overall higher correlations in the gray matter in comparison to the white matter. Figures 2 and 3 and Table 1 also show that the gray matter T2 tends to correlate more strongly with the higher EEG frequencies (e.g., α and β) than does the white matter while the white matter T2 relaxation times tended to be more strongly correlated with the lower EEG frequencies (e.g., δ, 0.5 to 3.5 Hz) than did those of the gray matter.

Relations between T2 Relaxation Times and Neuropsychological Tests

The previous analyses showed a correlation between gray matter and white matter T2 relaxation times and the EEG frequency spectrum. However, the clinical or functional relevance of these correlations is unclear. In order to investigate the behavioral meaning of the findings the relationship between T2 relaxation times and the severity of cognitive dysfunction was studied. A MANOVA with gray matter T2 and white matter T2 as factors and neuropsychological test scores as the dependent variables was conducted (Velleman, 1995). The MANOVA main effect of T2 and neuropsychological test scores was statistically significant ($df = 4$, $F = 14.5$, $P < 0.00001$). Statistically significant T2 relaxation

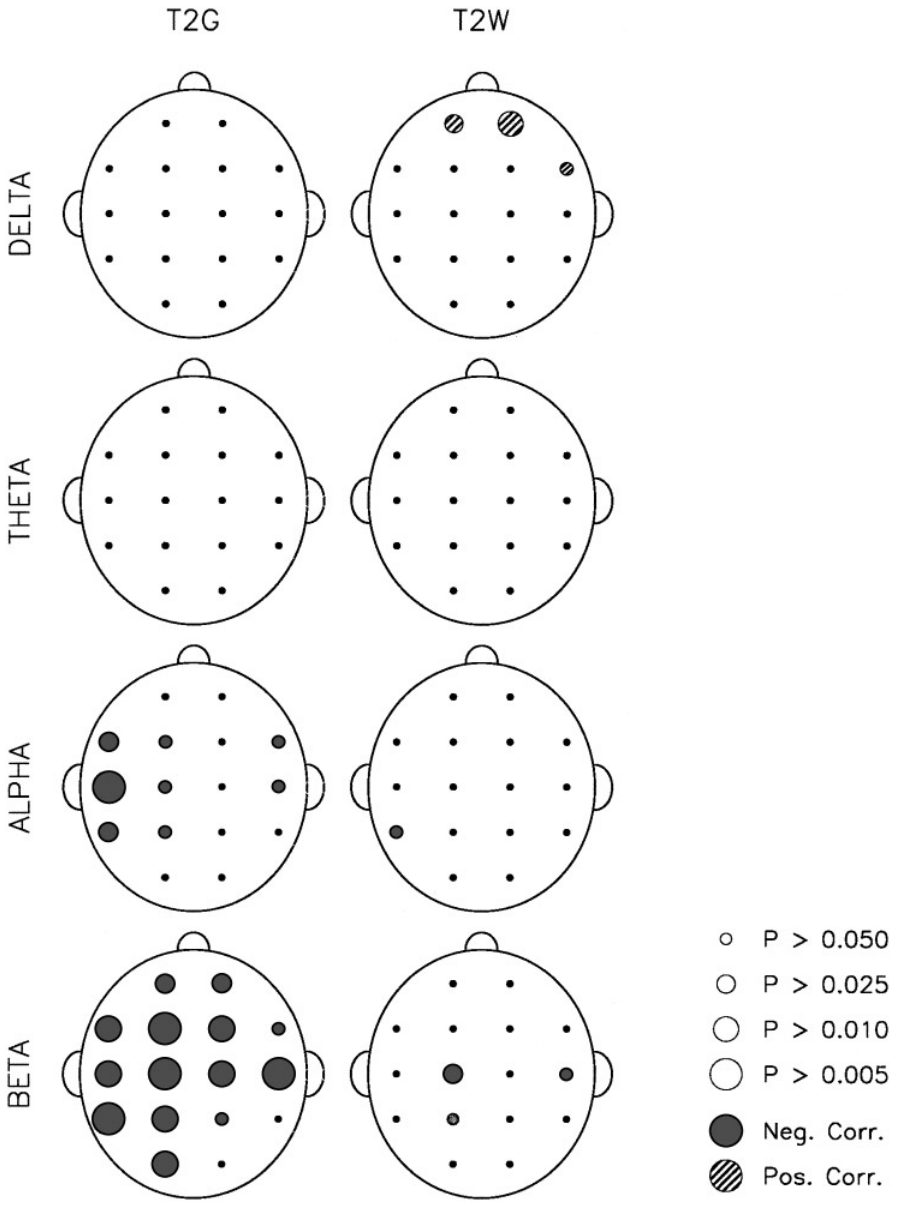

FIG. 5. Topographic analysis of EEG amplitude and T2 relaxation times. A topographic display of the magnitude of Bonferroni adjusted correlations between T2 relaxation time (independent variable) and $\log_{10}$ EEG amplitude (dependent variable) in the δ (0.5–3.5 Hz), θ (3.5–7 Hz), α (7–13 Hz), and β (13–22 Hz) frequency bands. Solid circle represents a negative or inverse relationship between T2 relaxation time and EEG amplitude while the striped circle represents a positive relationship between T2 relaxation time and EEG amplitude. The larger the diameter of the circle, the lower the probability value.

time effects were present for all of the neuropsychological tests. Table 2 summarizes the intercorrelations between the gray and the white matter T2 relaxation times and cognition as measured by performance on the neuropsychological tests. As was the relationship to EEG amplitude, T2 relaxation time was inversely related to neuropsychological performance. That is, increased T2 relaxation times were related to reduced cognitive function as measured by the neuropsychological test. Figure 7 shows representative regression scattergrams between neuropsychological tests and T2 relaxation time. The relationships tended to be well behaved; however, the number of test scores was relatively small.

Differences between neuropsychological test performance and gray versus white matter T2 relaxation times were also observed. As seen in Table 2, white matter T2 was not significantly related to digit span backward or to digit span raw score, whereas gray matter T2 was significantly related. However, caution should be exercised in evaluating the details of these findings because of the relatively small number of

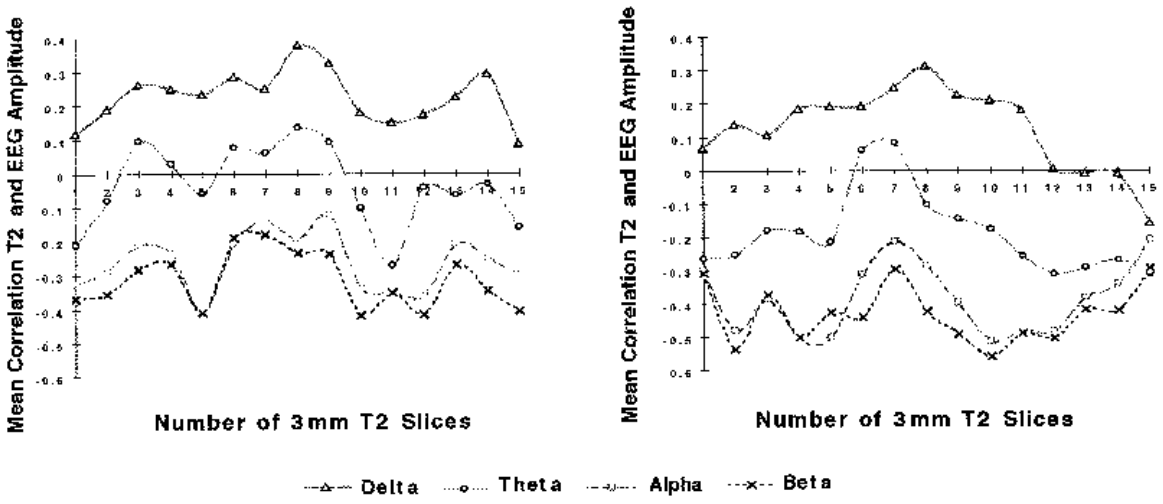

FIG. 6. T2 and EEG spatial correlations (4.5 cm). Mean correlation between T2 relaxation times and EEG amplitude at different frequencies summed across all EEG leads in the segmented white matter (left) and gray matter (right) of the 19 TBI patients. The *x* axis represents the 3-mm slices from 1 to 15 with slice 1 at the level of the genu and splenium of the corpus callosum. Slices 1 to 15 represent a contiguous spatial volume of 4.5 cm (i.e., 3 mm × 15 = 4.5 cm) beginning from the starting slice and extending to the top of the cortex (Thatcher *et al.,* 1997). A similar frequency relationship between EEG and T2 was present in the white and gray matter in which the δ frequency was positively correlated and the α and β frequencies were negatively correlated. The θ EEG frequency was only weakly correlated with T2 (see Table 1). Differences in the magnitude of T2 vs EEG correlations were present in different slice levels, e.g., slices 4 and 10 were most strongly correlated in the β frequency band and slice 8 was more strongly correlated in the δ frequency band. In general, β EEG frequencies were more strongly correlated with T2 gray matter while the δ EEG frequency band was more strongly correlated with T2 white matter (see Table 1).

subjects and the known "measurement variance" of neurospsychological tests (Levin *et al.,* 1982). The neuropsychological tests were only used to estimate the general level of cognitive function in this population of CHI patients.

Relations between EEG Amplitude and Neuropsychological Test Performance

A MANOVA with EEG amplitude in the four frequency bands from the 16 electrode locations as factors and neuropsychological test scores as the dependent variables was conducted (Velleman, 1995). The MANOVA main effect of EEG amplitude and neuropsychological test scores was statistically significant ($df = 15$, $F = 15.2$, $P < 0.00001$). As seen in Table 3, the lower EEG frequencies (i.e., δ and θ) exhibited an inverse canonical correlation with neuropsychological function while the higher EEG frequencies (i.e., α and β) were positively correlated with the level of neuropsychological function. Figure 8 shows examples of scattergrams and regression analyese between cognitive function and EEG amplitude.

TABLE 2

Number of Significant Correlations ($P < 0.05$) between Neuropsychological Performance, T2 Relaxation Time, and EEG Amplitude[a]

	Neuropsychological tests			
	Digit span backward	Digit span raw score	Calif. Verb. Learning	Boston Naming
T2—white	0	0	3	8
T2—gray	5	7	1	6

[a] One statistically significant correlation ($P < 0.05$) in each cell is expected to occur by chance alone.

DISCUSSION

The results of this study demonstrated statistically significant relations between MRI-derived T2 relaxation times and EEG amplitude in which increased relaxation times were related to: (1) decreased EEG amplitude in the α (7–13 Hz) and β (13–22 Hz) frequency bands, which was most strongly related to cortical gray matter T2 relaxation time, and (2) increased EEG δ (0.5–3.5 Hz) amplitude, which was most strongly related to the white matter T2 relaxation time. These effects were not correlated with the interval of time between injury and MRI test nor with edema and acute injury effects. Instead, the results of this study appear to be related to the chronic consequences of closed head injury.

Biomechanical studies of closed head injury have shown that fluid dynamic tissue boundaries determine the physical consequences of forces imparted to the human skull (Ommaya, 1968, 1995; Holbourn, 1943).

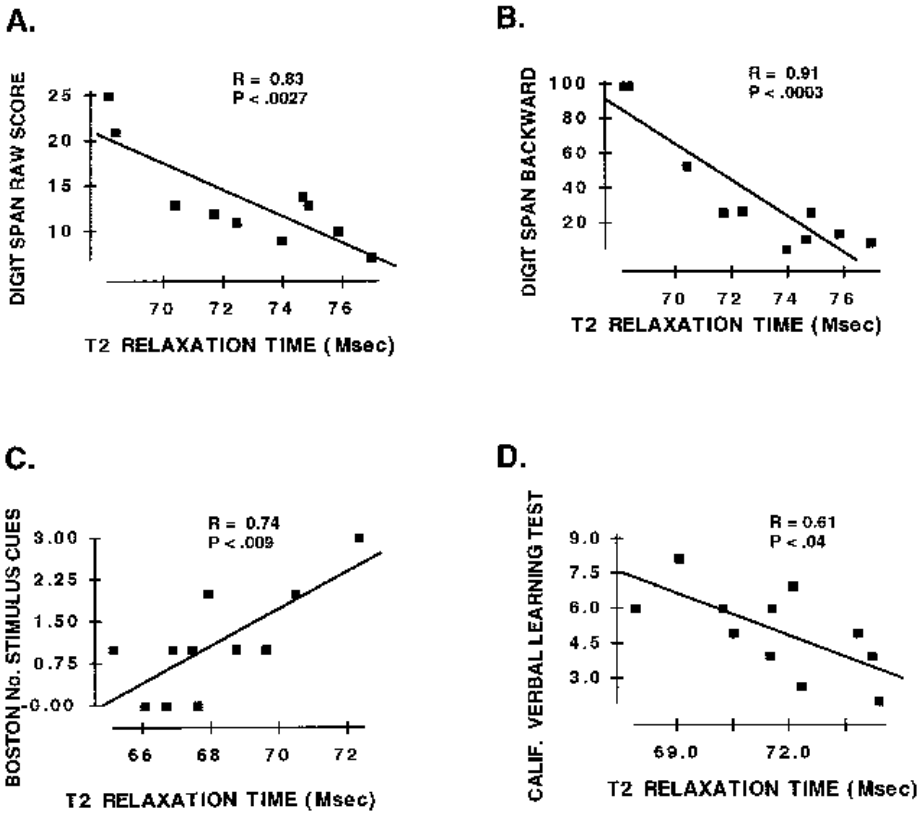

FIG. 7. T2 relaxation time and cognitive function. Representative scattergrams between different neuropsychological test scores (y axis) and T2 relaxation times (x axis). (A) Scattergram from slice 12 gray matter (x axis) and digit span raw score (WISC-R) (y axis). (B) Scattergram from slice 11 gray matter (x axis) and percentage of correct recall of digits in the digit span backward (WISC-R) (y axis). (C) Scattergram from slice 11 gray matter (x axis) and number of stimulus cues given in the Boston Naming test (y axis). (D) Scattergram from slice 11 gray matter (x axis) and the California Verbal Learning test (List A, trials 1–5) (y axis).

The majority of biomechanical studies over the past 30 years support a "centripetal" force vector which is maximum at the outer cortex with a gradient to the subcortex and brain stem (Ommaya, 1995), a rotational vector (Holbourn, 1943, 1945; Lee and Advani, 1970), and a shear vector (Advani *et al.,* 1982; Ommaya *et al.,* 1994). The geometrical summation of these forces results in maximum injury in that part of cortex that is in contact with the skull, e.g., the gray matter of the frontal and temporal lobes, which largely occurs independent of the direction of impact to the skull (Ommaya, 1995; Sano *et al.,* 1967). Two other invariant consequences of blunt force injuries to the skull are: (1) shear forces which are maximal at the boundaries between different densities of tissue (e.g., gray vs white matter) and (2) a percussion shock wave that travels from the point of impact, making contact with the opposite side of the skull in <200 ms, resulting in a "coup countre-coup" injury (Ommaya, 1995; Sano *et al.,* 1967). All of these forces are capable of seriously

TABLE 3

Results of Multivariate Analysis of Variance with Neuropsychological Tests as Dependent Variables and EEG Frequency as Factors

	Digit span backward		Digit span raw score		Calif. Verbal Learning		Boston Naming	
	t ratio	Prob.	t ratio	Prob.	t ratio	Prob.	t ratio	Prob.
δ	−3.46	0.001	−3.079	0.0031	−2.927	0.0048	−1.50	0.1388
θ	0.3232	0.7476	−0.5035	0.6165	−4.43	0.0001	6.054	0.0001
α	1.049	0.2984	0.8285	0.4107	3.177	0.0024	−0.1598	0.8735
β	2.087	0.0411	2.754	0.0078	4.181	0.0001	−4.394	0.0001

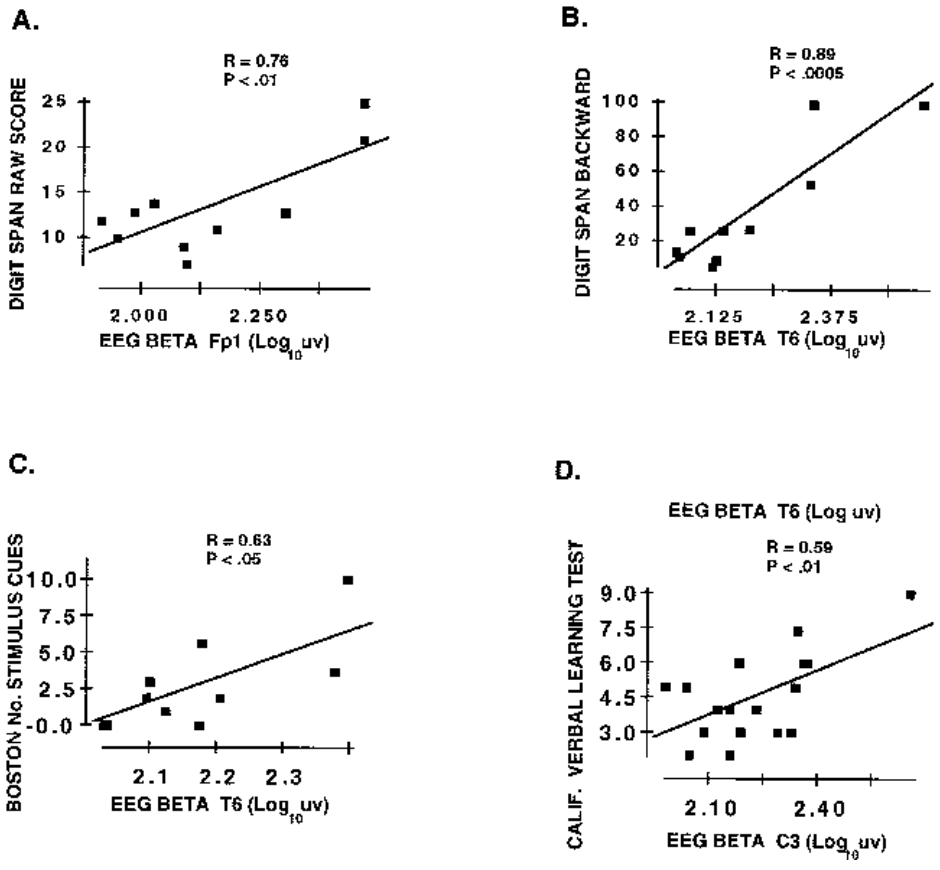

FIG. 8. EEG amplitude and cognitive function. Representative scattergrams between different neuropsychological test scores (*y* axis) and EEG amplitude (*x* axis). (A) Scattergram for Fp1 EEG β amplitude (*x* axis) and digit span raw score (WISC-R) (*y* axis). (B) Scattergram for T6 EEG β amplitude (*x* axis) and the percentage of correct score for digit span backward (*y* axis). (C) Scattergram for T6 EEG β amplitude (*x* axis) and the number of correct responses in the Boston Naming test (*y* axis). (D) Scattergram for C3 EEG β amplitude (*x* axis) and the California Verbal Learning test (List A, trials 1–5) (*y* axis).

disrupting the molecular integrity and function of cortical neurons and glia (Povlishock and Coburn, 1989).

Correlation between T2 Relaxation Time and Clinical EEG

The finding of increased EEG δ amplitude related to white matter T2 relaxation times and decreased β amplitude related to gray matter T2 relaxation times parallels clinical EEG findings involving lesions of the white matter compared to lesions of the gray matter (Gloor *et al.,* 1968, 1977; Goldensohn, 1979a,b; Schaul *et al.,* 1978). For example, increased δ EEG amplitude is a commonly reported clinical EEG correlate of white matter damage (Jasper and van Buren, 1953; Gloor *et al.,* 1968, 1977). Similarly, decreased β EEG amplitude is a common clinical correlate of gray matter damage (Gloor *et al.,* 1968, 1977; Goldensohn, 1979a,b). Gloor *et al.* (1977) studied this distinction between gray and white matter in cats in which he selectively destroyed either gray or white matter and consistently observed increased δ (1–4 Hz) following white matter lesions and decreased EEG high frequencies following gray matter lesions. Barlow (1993) explains the clinical EEG correlates of increased EEG δ by white matter damage and decreased β by gray matter damage in terms of the balance of excitatory and inhibitory drives that impinge on the cortex over some interval of time. For example, it is estimated that the vast majority of axons in the white matter are excitatory with terminations located primarily in different cortical layers, depending on their point of origin (Braitenberg, 1972, 1978; Nunez, 1981, 1995; Lopes da Silva, 1991). This is important because it follows that damage to the white matter must result in reduced excitatory input to the neocortex. In contrast, it is known that neocortical inhibitory synaptic inputs are generated by local interneurons at very short distances (e.g., <1 mm) and not by long-distance sources (Braitenberg, 1972, 1978; Nunez, 1981, 1995; Lopes da Silva, 1991). Thus, one would expect that injury to the white matter would reduce excitatory inputs to the neocortex, resulting in increased δ activity, while injury to the gray matter would reduce local or short-distance excitatory input to interneurons and

other pyramidal cells resulting in reduced amplitude of the EEG (Barlow, 1993). Another hypothesis is that damage to the gray matter not only reduces local excitation, but most importantly reduces synchronization of active generators, which in turn results in reduced surface-recorded EEG amplitude. This is certainly possible, especially when mathematical calculations show a highly disproportionate (e.g., >8:1) contribution to surface EEG amplitude by small groups of synchronous generators (e.g., Lopes da Silva, 1991; Cooper *et al.,* 1981; Nunez, 1981, 1995).

Although the precise biophysical mechanisms of lengthening T2 are unknown, a generic mathematical expression to numerically fit the EEG frequency spectrum to T2 relaxation time, independent of whether there are changes in the number of generators and/or their synchrony, is

$$\mathrm{EEG}_{\mathrm{amp}(f)} = A_1 e^{k_1 \mathrm{T2_w}} + A_2 e^{-k_2 \mathrm{T2_G}}, \qquad (2)$$

where A_1 and A_2 are low-frequency (0.5 to 3.5 Hz) and high-frequency (13 to 22 Hz) coefficients, respectively; k_1 and k_2 are constants; T2 is the T2 relaxation time mode of the white and gray matter, respectively, as defined by the solution of the Bloch equations (i.e., Eq. (1)), where I_{T2} and I_{PD} are the pixel intensities from the respective T2 and PD images); and amp(f) is the EEG amplitude spectrum in μV/cycle/s. The mathematical generality of the sum of two exponentials and the significant regression fit of this model to the EEG frequency spectrum established the usefulness of this expression.

Hypothesized Biophysical Linkage between MRI and EEG Amplitude

An experimentally demonstrated causal linkage between T2 relaxation time and EEG amplitude was not provided in the present study and additional experimentation specifically addressed to this issue is necessary before such a relationship can be established. However, the presentation of testable hypotheses not only facilitates future experimental design but also provides plausable explanations of the results observed in this study. For example, in the present study at least two testable hypotheses can explain all or most of the observed correlations: (1) A neuronal death or cell loss hypothesis. That is, as neurons are lost, the relative fraction of water protons in the intracellular compartment goes down and the relative fraction of water in the extracellular space goes up, resulting in lengthened T2 relaxation times as well as reduced EEG amplitude. (2) A membrane integrity hypothesis. That is, lengthened T2 relaxation time is due to a disruption in the integrity of the protein/lipid membranes of neurons, resulting in increased membrane permeability to water and a shift in the relative concentration of water between the intracellular and the extracellular compartments, which may occur independent of actual cell loss. According to the second hypothesis a spectrum of magnitude of injury to neurons, from subtle membrane disruption to cell death, results in a reduction in the efficacy of ionic membrane transport of neurons and, thus, reduced amplitude of EEG.

These hypotheses can be illustrated using standard compartmental models of T2 relaxation time (Szafer *et al.,* 1995; Kroeker and Henkelman, 1986; van Zijl *et al.,* 1991; Does and Snyder, 1995). According to compartmental models water protons are in dynamic interchange between different compartments: (1) axoplasm, (2) myelin, and (3) extracellular space. Proton density is a measure of the total number of water protons within these three compartments, which is measured immediately after the first 90° RF pulse when the water protons are tightly synchronous and have not interacted with their spin–spin (T2) and spin–lattice (T1) microenvironments. Shortly after the 90° RF pulse, T1 and T2 microenvironment effects occur. T1 represents relatively long processes (e.g., 200 to 4000 ms) which involve a time average over the various compartment exchanges, whereas T2 is shorter (20 to 150 ms) and more sensitive to the relative concentrations of water protons within these three compartments (Szafer *et al.,* 1995).

As shown in Fig. 9A, the three water proton microenvironments can be mathematically defined in terms of the total concentration of water protons [^{1}H] where [^{1}H] = [I] + [M] + [E], and [I] is defined as the concentration of intracellular water protons within the cortical cytoplasm (i.e., within the cytoplasm of the glia, axons, and neural dendrites and cell bodies), [M] is defined as the concentration of water protons within the cortical myelin, and [E] is defined as the concentration of water protons that are in the extracellular space, e.g., cerebral spinal fluid and the very small spaces between axons and neurons and between glia and neurons (Nicholson, 1980; Nicholson and Phillips, 1981). A diagrammatic illustration of the Bloch equation (Bloch, 1946) is shown in Fig. 9B. As depicted in Fig. 9B, the total concentration of water protons [^{1}H] is defined as the PD, which is a measure of the total number of water protons within all three compartments and is relatively independent of exactly which microenvironment in which the water atoms are located. As mentioned, T2 or spin–spin relaxation time is dependent on the frequency heterogeneity of the molecular microenvironment in which the water protons are embedded following the 90° RF pulse (Fullerton, 1992; Wehrli, 1992). The more homogeneous the spin frequencies are to the water proton spin frequency, the longer the T2 relaxation times; conversely, the more out-of-

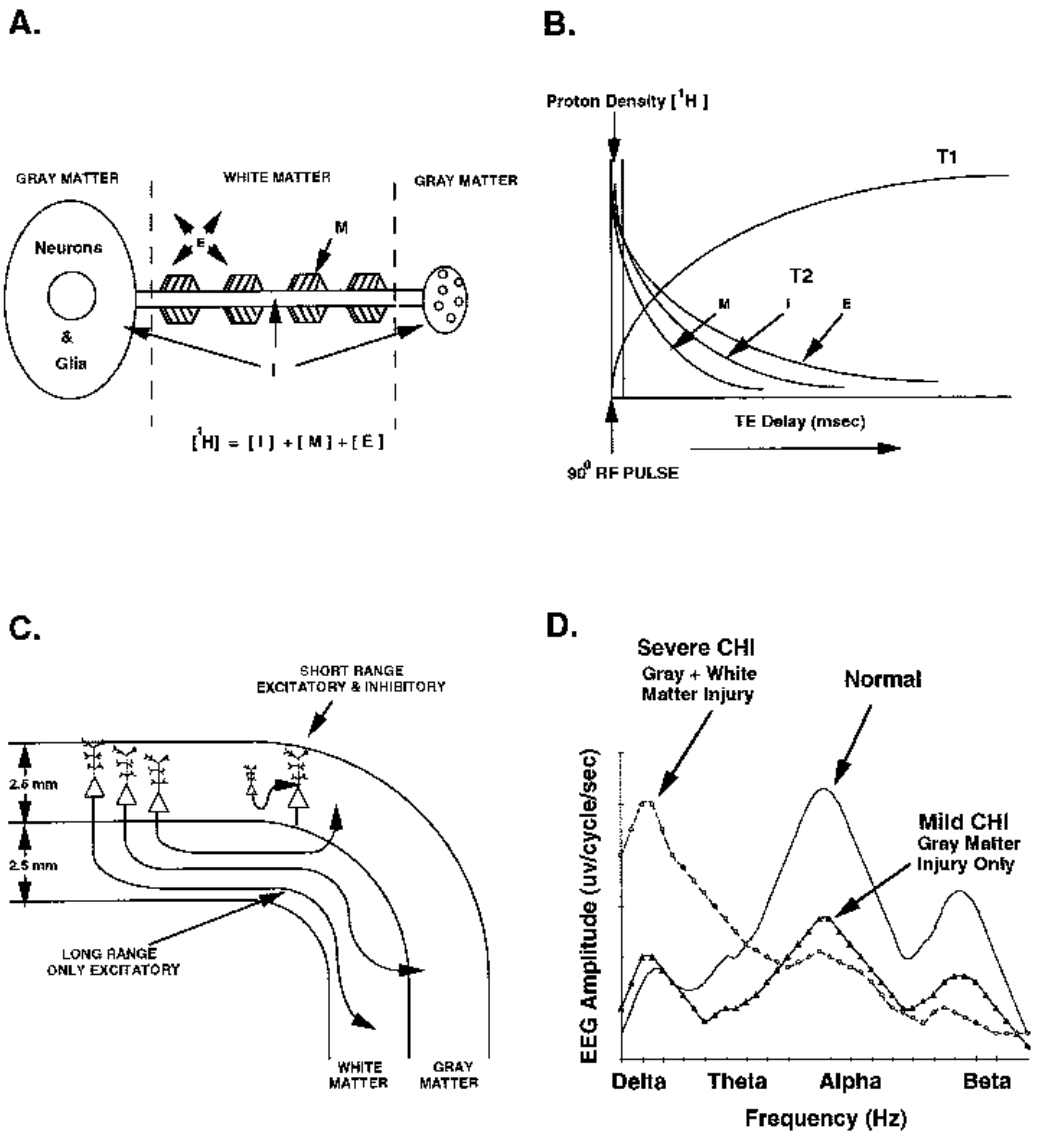

FIG. 9. Water proton microenvironment model for the CNS. Biophysical linkage of QMRI and QEEG. (A) Diagrammatic representation of a cortical neuron illustrating the distribution of water protons within the gray matter containing cell bodies, dendrites, and terminal butons (and glial cells) (I); the white matter containing axons and myelin (M); and extracellular space (E). The total concentration of water protons is mathematically represented as $[^1H] = [I] + [M] + [E]$, where $[^1H]$ is equal to the sum of water protons within the cytoplasm of neurons, glia, and axons (I) plus water protons within the myelin (M) plus water protons within the extracellular space (E). (B) Illustrative and diagrammatic representation of the NMR procedure of the conventional spin-echo in which at the moment of the 90° RF pulse the water protons in all three compartments have the same spin frequencies and are directly proportional to the proton density MRI measures (i.e., short TE and long TR). Immediately after the 90° RF pulse the water protons begin to interact with their different local environments, resulting in different T1 and T2 relaxation times. The shortest T2 relaxation times are from water protons in the myelin (M), the next longest T2 relaxation times are from water protons in the cytoplasm or intracellular space (I), and the longest T2 relaxation times are from water protons in the extracellular space (E). (C) Diagrammatic illustration of the neocortical white matter and gray matter where long-distance and myelinated axons travel and which exclusively exhibit excitatory input to the various layers of the neocortex. In contrast, the short-distance connections of the gray matter are both excitatory and inhibitory (e.g., inhibition from interneurons) and the inhibitory interneurons do not send axons into the white matter. (D) Diagrammatic illustration of the EEG frequency spectrum of normals, mild CHI patients, and severe CHI patients. It is hypothesized that mild traumatic injury is primarily confined to the gray matter, resulting in reduced EEG amplitudes in many frequencies since both inhibitory and excitatory neurons are damaged. With increased mechanical force to the skull, then the white matter compartment is injured in addition to gray matter injury. As a consequence, reduced excitatory input to the cortex results in the enhancement of δ EEG frequencies which are often observed in severe CHI patients.

phase the environmental spin frequencies to the spin–spin frequencies of the water protons, the shorter the T2 relaxation time. Shorter T2 relaxation times are present in the myelin, in comparison to the cytoplasm, because fat molecules [e.g., cholesterol (Koenig, 1991)] are hydrophobic and exhibit very different spin frequencies from water protons, thus creating a more heterogeneous spin–spin microenvironment. In contrast, longer T2 relaxation times are present in the cytoplasm because of a larger concentration of water molecules and thus a more homogeneous spin–spin microenvironment (Fullerton, 1992; Wehrli, 1992; Bottomley *et al.,* 1984).

Figure 9C illustrates the short-distance excitatory–inhibitory connections within the gray matter and the excitatory connections of the white matter as discussed above. Figure 9D is a depiction of the hypothesized relationship between EEG frequency spectrum and injury to the gray matter and white matter as measured by T2 relaxation times. Injury to the gray matter reduces both excitatory and inhibitory synaptic inputs to cortical pyramidal cells, which results in decreased EEG amplitude, especially in the higher frequencies. Injury to the white matter only reduces the excitatory inputs to the neocortex, resulting in increased δ activity (Fig. 9C). According to this hypothesis, mild CHI with neuropsychological dysfunction may be identified as a gray matter injury with no or minimal white matter damage as depicted in Fig. 9D. With increased biomechanical force, a "centripetal" vector invades the white matter and subcortical structures (Ommaya, 1995) as reflected by increased δ EEG waves. This suggests that lengthened T2 and/or reduced relaxation contrast (Thatcher *et al.,* 1997) is due to injury to the gray and white matter with the distinction between hypotheses 1 and 2 being that of the extent of neuronal destruction. It is feasible to test these hypotheses by experimentally relating EEG amplitude to the apparent diffusion coefficient of water molecules in the cytoplasm versus the extracellular space of the brain as well as with measures of neuron-specific amino acids such as NAA in addition to T2 relaxation time (Szafer *et al.,* 1995; Le Bihan *et al.,* 1991; van Zijl *et al.,* 1991; Hsu *et al.,* 1996).

Relations between Cognition, EEG, and T2 Relaxation Times

The relevance of the findings in this study are emphasized by the fact that three independently obtained measures, MRI, EEG, and neuropsychological performance, significantly correlated with each other, suggesting a functional linkage. The linkage was evidenced by a consistent direction of correlation in which increased T2 relaxation times were correlated with decreased EEG α (7–13 Hz) and β (13–22 Hz) amplitude and declining cognitive performance, while decreased EEG α and β amplitude was also correlated with reduced cognitive performance. This suggests a linkage between the measure in which lengthened T2 of brain gray and white matter is related to cognition and EEG in CHI patients. That is, as the integrity of protein and/or lipid membranes of the gray and white matter is reduced, the efficiency of neuronal function declines as reflected in declining cognitive function as well as in EEG amplitude change. However, a study with a larger number of subjects than in the present study is necessary to more fully understand the relationship between neuropsychological functioning and MRI and EEG.

SUMMARY

The choice of a CHI patient cohort for this study offered the advantage of a broader spectrum of pathology and cognitive test scores than expected in a normal control group and, thus, a greater probability of demonstrating the correlations that we found. However, it is not clear whether these findings are unique to CHI or also present in normal individuals. It is also unknown if similar findings will be observed between T2 and EEG as a function of aging or in brain pathologies other than CHI. The spatial resolution of these effects has also not been tested. The main purpose of this study was to establish the feasibility of linking MRI biophysical measures of water protons to the EEG of traumatic brain injured patients. Even if only observed in CHI patients, the fact that MRI relaxation times can be related to the scalp-recorded EEG is significant. Such a linkage may expand our understanding of the genesis of the electroencephalogram and aid in the integration of EEG, MRI, and cognition.

APPENDIX

The calculation of T2 relaxation time is based on the fact that $TR_{T2} = TR_{PD}$, thus

$$\frac{I_{T2}}{I_{PD}} = \frac{KN(1 - e^{-TR_{T2}/T1})e^{-TE_{T2}/T2}}{KN(1 - e^{-TR_{T2}/T1})e^{-TE_{PD}/T2}}; \quad (1)$$

since K, N, and TR_{PD} cancel, Eq. (1) can be simplified to

$$\frac{I_{T2}}{I_{PD}} = \frac{e^{TE_{PD}-TE_{T2}}}{T2}, \quad (2)$$

The solution for T2 is obtained by taking the log of the ratio, of

$$\ln\left(\frac{I_{T2}}{I_{PD}}\right) = \frac{TE_{PD} - TE_{T2}}{T2}, \quad (3)$$

and then by rearranging to solve for T2,

$$T2 = \frac{TE_{PD} - TE_{T2}}{\ln(I_{T2}/I_{PD})}, \quad (4)$$

where I_{T2} and I_{PD} are the pixel intensities from the respective T2 and PD images.

ACKNOWLEDGMENTS

We acknowledge the data analysis and editorial assistance of Rebecca Walker, Richard Curtin, Dr. William Hudspeth, and Duane North. We are also indebted to Drs. Glen Curtis, Rodney Vanderploog, and Rex Bierley for discussions of the neuropsychological tests, Ms. Kathleen Haedt for administering the neuropsychological tests, and Dr. Joseph Green for discussions of clinical EEG. This project was supported by Contract JFC36285006 as part of the Defense and Veterans Head Injury Program. Informed consent was obtained from all patients in this study.

REFERENCES

Adams, J. H., Doyle, D., Ford, I., Gennarelli, T. A., Graham, D. I., and McLellan, D. R. 1989. Diffuse axonal injury in head injury: Definition, diagnosis and grading. *Histopathology* **15:**49–59.

Advani, S. H., Ommaya, A. K., and Yang, W. J. 1982. Head injury mechanisms, characteristics and clinical evaluation. In *Human Body Dynamics* (D. Chista, Ed.), *Oxford Medical Engineering Series,* pp. 3–37 Clarendon, Oxford.

Barlow, J. S. 1993. *The Electroencephalogram: Its Patterns and Origins.* MIT Press, Cambridge, MA.

Bensaid, A. M., Hall, L. O., Bezdek, J. C., and Clarke, L. P. 1994. Fuzzy cluster validity in magnetic resonance images. In *Medical Imaging 1994: Image Processing.* (M. H. Loew, Ed.), *Proceedings SPIE* 2167, pp. 454–464. Int. Soc. Opt. Eng., Bellingham, WA.

Bezdek, J. C., Hall, L. O., and Clarke, L. P. 1993. Review of MR image segmentation techniques using pattern recognition. *Med. Phys.* **20:**1033–1048.

Bloch, F. 1946. Nuclear induction. *Phys. Rev.* **70:**460–482.

Bottomley, P. A., Foster, T. H., Argersinger, R. E., and Pfeifer, L. M. 1984. A review of normal tissue hydrogen NMR relaxation times and relaxation mechanisms from 1–100 MHz: Dependence on tissue type, NMR frequency, temperature, species, excision and age. *Med. Phys.* **11:**425–448.

Bottomley, P. A., Hardy, C. J., Argersinger, R. E., and Allen-Moore, G. 1987. A review of ^{1}H nuclear magnetic resonance relaxation in pathology: Are T_1 and T_2 diagnostic? *Med. Phys.* **14:** 1–36.

Braitenberg, V. 1972. Comparison of different cortices as a basis for speculation on their function. In *Synchronization of EEG Activity in Epilepsies* (H. Petsche and M. Brazier, Eds.), pp. 47–63 Springer-Verlag, New York.

Braitenberg, V. 1978. Cortical architectonics: General and areal. In *Architectonics of the Cerebral Cortex* (M. Brazier and H. Petsche, Eds.), pp. 443–465. Raven Press, New York.

Carpender, M. B., and Sutin, J. 1983. *Human Neuroanatomy,* 5th ed. Williams & Wilkins, Baltimore.

Clarke, L. P., Velthuizen, R. P., Camacho, M. A., Heine, J. J., Vaidyanathan, M., Hall, L. O., Thatcher, R. W., and Silbiger, M. L. 1995. MRI segmentation: Methods and applications. *Magn. Reson. Imaging* **13:** 343–368.

Cohen, J., and Cohen, P. 1983. *Applied Multiple Regression/Correlation Analysis for the Behavioral Sciences.* Erlbaum, Hillsdale, NJ.

Cooper, R., Osselton, J. W., and Shaw, J. C. 1981. *EEG Technology,* 3rd ed. Butterworth, Stoneham, MA.

Darwin, R. H., Drayer, B. P., Riederer, S. J., Wang, H. Z., and MacFall, J. R. 1986. T2 estimates in healthy and diseased brain tissue: A comparison using various MR pulse sequences. *Radiology* **160:** 375–381.

Dixon, R. L., and Ekstrand, K. E. 1982. The physics of proton NMR. *Med. Phys.* **9:**807–818.

Does, M. D., and Snyder, R. E. 1995. T2 relaxation of peripheral nerve measured in vivo. *Magn. Reson. Imag.* **13:**575–580.

Fullerton, G. D. 1992. Physiological basis of magnetic relaxation. In *Magnetic Resonance Imaging* (D. D. Stark and W. G. Bradley, Eds.), pp. 88–108. Mosby, St. Louis.

Gentry, L. R. 1990. Head trauma. In *Magnetic Resonance Imaging of the Brain and Spine* (S. W. Atlas, Ed.), pp. 439–466. Raven Press, New York.

Gentry, L. R. 1994. Imaging of closed head injury. *Radiology* **191:** 1–17.

Gentry, L. R., Godersky, J. C., and Thompson, B. 1988. MR imaging of head trauma: Review of the distribution and radiopathologic features and traumatic lesions. *Am. J. Radiol.* **150:**663–672.

Gloor, P., Ball, G., and Schaul, N. 1977. Brain lesions that produce delta waves in the EEG. *Neurology* **27:**326–333.

Gloor, P., Kalabay, O., and Giard, N. 1968. The electroencephalogram in diffuse encephalopathies: Electroencephalographic correlates of grey and white matter lesions. *Brain* **91:** 779–802.

Goldensohn, E. S. 1979a. Use of the EEG for evaluation of focal intracranial lesions. In *Current Practice of Clinical Electroencephalography* (D. Klass and D. Daly, Eds.). Raven Press, New York.

Goldensohn, E. S. 1979b. Neurophysiologic substrates of EEG activity. In *Current Practice of Clinical Electroencephalography* (D. Klass and D. Daly, Eds.). Raven Press, New York.

Graham, D. J., Adams, J. H., and Gennarelli, T. 1993. Pathology of brain damage. In *Head Injury* (P. R. Cooper, Ed.), 3rd ed., Williams & Wilkins, Baltimore.

Hickley, D. S., Checkleyt, D., Aspden, R. M., Naughton, A., Jenkins, J. P., and Isherwood, I. 1986. A method for the clinical measurement of relaxation times in magnetic resonance imaging. *Br. J. Radiol.* **59:** 565–576.

Holbourn, A. H. S. 1943. Mechanics of head injuries. *Lancet* **2:**438–441.

Holbourn, A. H. S. 1945. The mechanics of brain injuries. *Br. Med. Bull.* **3:**147–149.

Hus, E. W. Aiken, N. R., and Blackband, S. J. 1996. Nuclear magnetic resonance microscopy of single neurons under hypotonic perturbation. *Am. J. Physiol. (Cell Physiol.)* **40:**C1895–C1900.

Jasper, H., and van Buren, J. 1953. Interrelationship between cortex and subcortical structures: Clinical electroencephalographic studies. *Electroencephalogr. Clin. Neurophysiol. (Suppl).* **4:**168–188.

Kjos, O., Ehman, R. L., Brant-Zawadzki, M., Kelly, W. M., Normasn, D., and Newton, T. H. 1985. Reproducibility of relaxation times and spin density calculated from routine MR imaging sequences: Clinical study of the CNS. *Am. J. Radiol.* **144:**1165–1170.

Koenig, S. H. 1991. Cholesterol of myelin is the determinant of gray–white contrast in MRI of brain. *Magn. Reson. Med.* **20:**285–291.

Kroeker, R. M., and Henkelman, R. M. 1986. Analysis of biological NMR relaxation data with continuous distributions of relaxation times. *J. Magn. Reson.* **69:**218–235.

Le Bihan, D., Turner, R., Moonen, C. T. W., and Pekar, J. 1991. Imaging of diffusion and microcirculation with gradient sensitization: Design, strategy and significance. *J. Magn. Reson. Imaging* **1:**7–28.

Lee, Y. C., and Advani, S. H. 1970. Transient response of a sphere to symmetric torsional loading: A head injury model. *Math. Biosci.* **6:**473–487.

Levin, H. S., Benton, A. I., and Grossman, R. G. 1982. *Neurobehavioral Consequences of Closed Head Injury.* Oxford Univ. Press, New York.

Lopes da Silva, F. H. 1991. Neural mechanisms underlying brainwaves: From neural membranes to networks. *Electroencephalogr. Clin. Neurophysiol.* **79:**81–93.

Mills, C. M., Crooks, L. E., Kaufman, L., and Brant-Zawadzki, M. 1984. Cerebral abnormalities: Use of calculated T1 and T2 magnetic resonance images for diagnosis. *Radiology* **150:**87–94.

Nicholson, C. 1980. Dynamics of the brain cell microenvironment. *Neurosci. Res. Program Bull.* **18**(2):181–243.

Nicholson, C., and Phillips, J. M. 1981. Ion diffusion modified by tortuosity and volume fraction in the extracellular microenvironment of the rat cerebellum. *J. Physiol.* **321:**225–257.

Nunez, P. 1981. *Electrical Fields of the Brain.* Oxford Univ. Press, Cambridge, UK.

Nunez, P. 1995. *Neocortical Dynamics and Human EEG Rhythms.* Oxford Univ. Press, New York.

Ommaya, A. K. 1968. The mechanical properties of tissues of the nervous system. *J. Biomech.* **2:**1–12.

Ommaya, A. K. 1995. Head injury mechanisms and the concept of preventive management: A review and critical synthesis. *J. Neurotrauma* **12:**527–546.

Ommaya, A. K., Thibault, L. E., and Bandak, F. A. 1994. Mechanisms of impact head injury. *Int. J. Impact Eng.* **15**(4):535–560.

Otnes, R. K., and Enochson, L. 1972. *Digital Time Series Analysis*. Wiley, New York.

Povlishock, J. T., and Coburn, T. H. 1989. Morphopathological change associated with mild head injury. In *Mild Head Injury* (H. S. Levin, H. M. Eisenberg, and A. L. Benton, Eds.), pp. 37–53. Oxford Univ. Press, New York.

Sano, K., Nakamura, N., and Hirakaws, K. 1967. Mechanism of and dynamics of closed head injuries. *Neurol. Mediochir.* **9:**21–23.

Savitzky, A., and Golay, M. J. E. 1964. Smoothing and differentiation of data by simplified least squares procedures. *Anal. Chem.* **36:**1627–1639.

Schaul, N., Bloor, P., Ball, G., and Cotman, J. 1978. The electromicrophysiology of delta waves induced by systemic atropine. *Brain Res.* **143:**475–486.

Smith, D. H., Meaney, D. F., Lenkinski, R. E., Alsop, D. C., Grossman, R., Kimura, H., McIntosh, T. K., and Gennarelli, T. A. 1995. New magnetic resonance imaging techniques for the evaluation of traumatic brain injury. *J. Neurotrauma* **12:**573–578.

Szafer, A., Zhong, J., and Gore, J. C. 1995. Theoretical model for water diffusion in tissues. *Magn. Reson. Med.* **33:**687–712.

Thatcher, R. W. 1995. Tomographic electroencephalography and magnetoencephalography. *J. Neuroimaging* **5:**35–45.

Thatcher, R. W., Walker, R. A., Gerson, I., and Geisler, F. 1989. EEG discriminant analyses of mild head trauma. *Electroencephalogr. Clin. Neurophysiol.* **73:**93–106.

Thatcher, R. W., Cantor, D. S., McAlaster, R., Geisler, F., and Krause, P. 1991. Comprehensive predictions of outcome in closed head injury: The development of prognostic equations. *Ann. N. Y. Acad. Sci.* **620:**82–104.

Thatcher, R. W., Camacho, M., Salazar, A., Linden, C., Biver, C., and Clarke, L. 1997. Quantitative MRI of the gray–white matter distribution in traumatic brain injury. *J. Neurotrauma* **14:**1–14.

van Zijl, P. C. M., Moonen, C. T. W., Faustino, P., Pekar, J., Kaplan, O., and Cohen, J. S. 1991. Complete separation of intracellular and extracellular information in NMR spectra of perfused cells by diffusion weighted spectroscopy. *Proc. Natl. Acad. Sci. USA* **88:** 3228–3232.

Velleman, P. F. 1995. *Data Desk: Version 5.0.* Data Description, Inc., Ithaca, NY.

Wehrli, F. W. 1992. Principles of magnetic resonance. In *Magnetic Resonance Imaging* (D. D. Stark and W. G. Bradley, Eds.). pp.3–20. Mosby, St. Louis.